

# Growth of Nanocrystal Superlattices from Liquid Crystals

S. Yang, Y. Zhang

To be published in "Journal of the American Chemical Society"

April 2024

Center for Functional Nanomaterials  
**Brookhaven National Laboratory**

**U.S. Department of Energy**

USDOE Office of Science (SC), Basic Energy Sciences (BES). Scientific User Facilities (SUF)

Notice: This manuscript has been authored by employees of Brookhaven Science Associates, LLC under Contract No. DE-SC0012704 with the U.S. Department of Energy. The publisher by accepting the manuscript for publication acknowledges that the United States Government retains a non-exclusive, paid-up, irrevocable, world-wide license to publish or reproduce the published form of this manuscript, or allow others to do so, for United States Government purposes.

## **DISCLAIMER**

This report was prepared as an account of work sponsored by an agency of the United States Government. Neither the United States Government nor any agency thereof, nor any of their employees, nor any of their contractors, subcontractors, or their employees, makes any warranty, express or implied, or assumes any legal liability or responsibility for the accuracy, completeness, or any third party's use or the results of such use of any information, apparatus, product, or process disclosed, or represents that its use would not infringe privately owned rights. Reference herein to any specific commercial product, process, or service by trade name, trademark, manufacturer, or otherwise, does not necessarily constitute or imply its endorsement, recommendation, or favoring by the United States Government or any agency thereof or its contractors or subcontractors. The views and opinions of authors expressed herein do not necessarily state or reflect those of the United States Government or any agency thereof.

# Growth of Nanocrystal Superlattices from Liquid Crystals

Shengsong Yang<sup>1,‡</sup>, Yifan Ning<sup>1,‡</sup>, Yugang Zhang<sup>2</sup>, Christopher B. Murray<sup>1,3,\*</sup>

<sup>1</sup>Department of Chemistry, University of Pennsylvania, Philadelphia, Pennsylvania 19104, United States.

<sup>2</sup>Center for Functional Nanomaterials, Brookhaven National Laboratories, Upton, New York, 11973, United States.

<sup>3</sup>Department of Materials Science and Engineering, University of Pennsylvania, Philadelphia, Pennsylvania 19104, United States.

<sup>‡</sup>These authors contributed equally to this work.

\*Corresponding Author: cbmurray@sas.upenn.edu

## *Supporting Information Placeholder*

---

**ABSTRACT:** The growth of superlattices (SLs) made from self-assembled nanocrystals (NCs) is a powerful method for creating new materials and gaining insights into fundamental molecular dynamics. Previous explorations of NCSL syntheses have mostly compared it to crystallization. However, NCSL synthesis has not broadly shown cooling crystallization from saturated solutions as a reversible crystallization-dissolution process. We demonstrate the reversible growth of NCSLs by dispersing NCs in liquid crystal (LCs) “smart solvents,” and harnessing the transitions between the isotropic and nematic phases of the LCs. The growth mode and morphology can be tuned. This process is a model platform for studying crystallization and demonstrates great potential in manufacturing the NCSLs as colloidal crystals through liquid-phase epitaxy or colloidal synthesis.

---

The growth of well-ordered nanocrystal superlattices (NCSLs) opens avenues for developing materials with diverse chemical and physical characteristics.<sup>1-3</sup> These NCSLs, crafted from NC self-assembly, emulate crystalline structures and their constituent molecules, establishing a vital link between self-assembly and crystallization.<sup>4-8</sup> The solvent environment and tailored ligands significantly influence the growth of NCSLs.<sup>9-11</sup> Similarly to the crystallization of molecules and ions, the self-assembly of NCs commonly employs methods such as non-reversible solvent evaporation and solvent polarity manipulation using solvent-antisolvent pairs.<sup>12,13</sup> However, the straightforward method of cooling saturated solutions remains underreported in NCSL formation.<sup>14,15</sup> This limitation has hindered the manufacture of NCSLs and the purification of NCs by re-crystallization.<sup>16-18</sup> Previous demonstrations of reversible NC self-assembly near room temperature used responsive ligands such as DNA and its derivatives,<sup>13,19</sup> photo-switchable ligands,<sup>20</sup> and charged

ligands.<sup>21</sup> Analogously, more controlled NCSL growth can be achieved through the use of appropriate responsive ‘smart solvents,’ which promote the broad application of cooling crystallization in an optimum temperature window.<sup>22</sup> This approach brings a deeper understanding of the NCSL growth mechanism and enables shape-controlled NCSL growth, paving the way for the ‘colloidal synthesis’ of NCSLs.<sup>23-26</sup>

The unique supramolecular alignment of liquid crystals (LCs) has provided templates, or matrices, to induce the arrangement of NCs into pre-specified geometries.<sup>27-30</sup> Many previous studies focused on controlling the formation of these macroscopic structures,<sup>31-34</sup> yet there have been few reports on the growth mechanism of NCSLs obtained by cooling LCs. The crystalline yet fluidic nature of LCs makes them promising candidates for temperature-responsive smart solvents in atomic crystal fabrications<sup>35</sup> and NCSL self-assembly. In their isotropic phase, NCs can disperse,<sup>36</sup> resembling traditional solvents used in colloidal NC research; however, cooled LCs expel NCs,<sup>37,38</sup> which can drive NCs assembly into NCSLs.<sup>39,40</sup> Here, we use LCs as smart solvents to achieve a highly reversible growth of NCSL building upon our prior work on NC engineering<sup>4,41,42</sup> and surface engineering.<sup>5,43</sup> The temperature window for the growth and dissolution of NCSLs is determined by the intrinsic LC phase transition temperature. Two types of classical crystal growth mechanisms,<sup>44</sup> the island growth and the epitaxial growth, can be achieved by the dictation of ligands, leading to different NCSL structures. The yield of NCSLs from LCs is above 90%. We show that cooling crystallization of NCs from LCs enhances control over the NC self-assembly process compared to existing methods and can be potentially used in separation and purification.

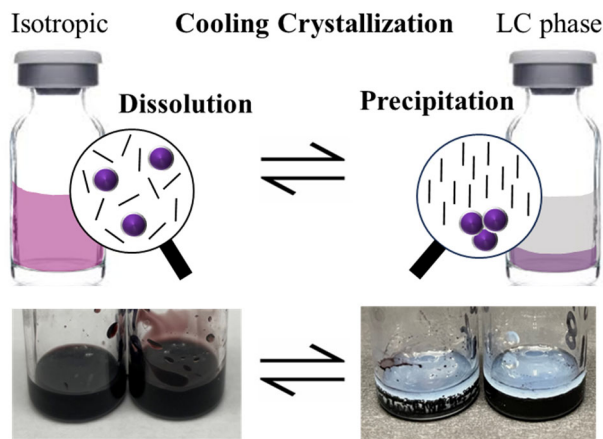


**Figure 1.** Schematics of the crystallization and dissolution of NCs triggered by the phase transition of LCs. 1.0 wt% of NCs in 5CB are shown in the figure.

A model system employing 5.0 nm diameter Au NCs as the solute and 4-cyano-4'-pentylbiphenyl (5CB) as the LC solvent was utilized to instigate the growth of NCSLs triggered by LC phase transition (Figure 1). Surface functionalization of NCs is essential to enable uniform dispersion of NCs in isotropic LCs, and our recent design of promesogenic ligands has proven effective for this process.<sup>43,45</sup> For consistency with our previous work, ligands used in this study are referred to using the same nomenclatures (Scheme S1). Small-angle X-ray scattering (SAXS) confirms NCs are dispersed in the isotropic phase and assembled in the nematic phase (Figure S2). The resulting isotropic LC dispersions closely resemble a dispersion of NCs in chloroform (Figure S3). Upon cooling to the transition temperature ( $T_{NI}$ ) of 5CB at 34 °C, the solubility of the NCs decreases by 90% with **L3** or even 99% with **L2** (Table S1). NCs aggregate, crystalize, and precipitate 'on demand' from the dispersion within 1 to 20 minutes. A uniform dispersion can be fully recovered by warming the system above  $T_{NI}$ . This process is solely induced by the transition of LCs, contributing to the superior reversibility of this method. This phenomenon is analogous to standard cooling crystallization, with NCs as colloidal solutes in a crystalline solvent. These features make the system a promising candidate for studying and understanding the crystallization process through in situ techniques at ideal temperatures and time scales.

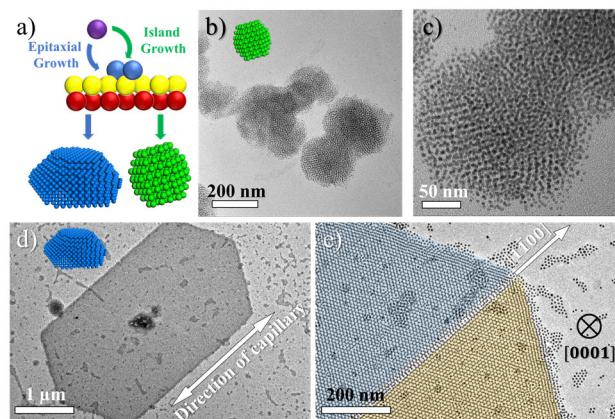


**Figure 2.** a) Schematics of different growth routes. b) and c) Corresponding TEM of Au-**L2** NCSLs. d) and e) Corresponding TEM of Au-**L3** NCSLs. Indices of the lattice axis adapt the hexagonal close pack (HCP) structure.

In any crystallization process, both thermodynamics and kinetics can alter the crystalline products. For example, shape-controlled NC syntheses are enabled by tuning the equilibrium between deposition and dissolution. The well-faceted crystals are found as thermodynamic products through epitaxial growth, where near-spherical clusters or crystals result as kinetic products of island growth or rapid aggregation.<sup>46</sup> In this work, we found similarities between the growth of NCSLs where NCs are considered as tunable artificial atoms. Such control over NSCL growth mode and morphology of NCSLs has not been reported using the solvent evaporation method.

Despite the identical appearance of sediments with visual inspection and optical microscopy, transmission electron microscopy (TEM) reveals that the presence of NCSLs with different crystal shapes grow from 5CB using two ligands (Figure 2a). **L2** and **L3** share similar dendritic structures and the same biphenyl functional groups as tails, yet they are different in their branched chains. Au-**L2** NCSLs predominantly adopt polyhedral crystal forms (Figure 2, b, and c). These NCSLs have dimensions smaller than one micrometer and exhibit random orientations (Figure S6). In contrast, layered NCSL flakes in an elongated hexagonal shape can be obtained from Au-**L3** when cooled from 5CB (Figure 2d). These flakes feature well-defined corners, sharp edges, and smooth facets, together resembling a single crystal with a size of several micrometers (Figure S7). The close-packed facets of the NCSLs consistently face up, and different NCSLs share the same elongated lattice axis. Grain boundaries are occasionally observed along the longer diagonal axis (Figure 2e). These diverse NCSL crystal shapes could represent different growth trajectories. The ligand structural difference is exaggerated by this liquid crystalline solvent.

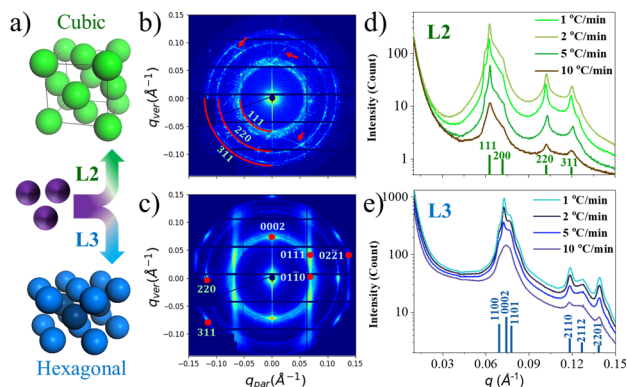


**Figure 3.** a) Scheme of different close-packed NCSL phases from different ligands. 2D SAXS pattern of (b) Au-L2 NCSLs grown in LCs and (c) Au-L3 NCSLs. Kossel lines are marked with arrows. Indices in blue indicate HCP and indices in green indicate FCC. The circulation average of SAXS results from different cooling rates of (e) Au-L2 and (f) Au-L3.

The formation and growth of NCSLs are tracked using in situ SAXS to elucidate the effects of different ligands on self-assembly behaviors (Figure 3a). Dispersions of 1.0 wt% of NCs in 5CB in capillaries are cooled from 45 °C to 18 °C with different rates. At the beginning, SAXS shows the form factors from uniform dispersion of Au-L2 and Au-L3 above  $T_{NI}$  (Figure S2). Au-L2 presents predominantly polycrystalline face-centered cubic (FCC) structures with Kossel patterns (Figure 3b), consistent with the TEM results. Au-L2 exhibits negligible variation in peak widths across different cooling rates (Figure 3d). In contrast, Au-L3 consistently produces a discrete, orientationally preferred pattern incorporating HCP mixed with FCC phases (Figure 3c). A narrower peak width from a slower cooling rate in Au-L3 NCSLs signifies the attainment of either a more refined crystalline structure or larger crystalline domains (Figure 3e). Rapid cooling (20 °C/min) of the dispersion may result in random aggregates (Figure S11). Additionally, Au-L3 NCSLs display a shorter interparticle distance compared to Au-L2 despite having a similar ligand length and grafting density.

This can be explained by the solubility of NCs during the growth process. Solubility of NCs first alters the equilibrium between dissolution and crystallization, leading to different crystal ripening and possibly different growth mechanisms.<sup>26</sup> In the nematic phase of 5CB, Au-L3 has better solubility than Au-L2 (Table S1). When Au-L3 clusters form and sediment, the better solubility provides NCs an opportunity for migration and reorientation to form large crystalline domains with fewer grain boundaries through ripening. In contrast, once the small crystalline Au-L2 clusters form at the interface between the isotropic and nematic domains of LCs, the poor solubility prevents NCs from dissolving or reordering. They therefore maintain their size and shape. Under TEM, random, free NCs consistently appear in the Au-L3 system but not in Au-L2. The small polyhedrons of Au-L2 align closely

with the kinetic product, whereas the thermodynamically favored, large NCSLs appear in Au-L3. Also, based on our prior studies of the lubricating phenomena without LC solvents, L3 results in less ligand interdigitation and better mobility for individual NCs in NCSLs than L2,<sup>47</sup> which could also facilitate the migration of Au-L3 NCs after deposition.

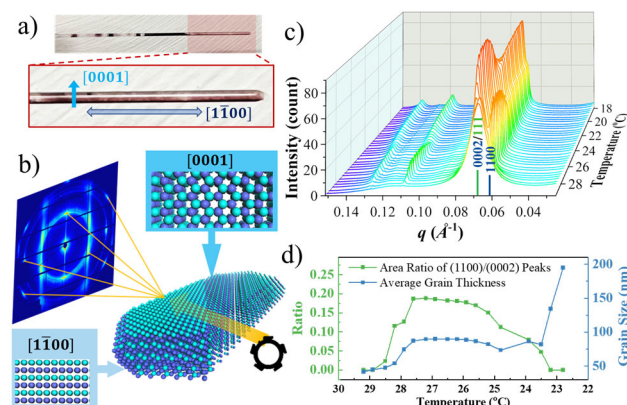


**Figure 4.** a) Sediments of Au-L3 NCSLs in a horizontally placed capillary with a diameter of 1.0 mm after the heating-cooling cycle. b) Corresponding demonstration of the Au-L3 NCSLs in capillaries and crystal orientation obtained from SAXS and TEM. c) In situ SAXS of superlattice growth during cooling crystallization. The indices are in blue for HCP peaks and green for FCC peaks. d) Peak evolving and vertical grain size change during epitaxial growth.

Our observation of orientational alignment in SAXS and TEM of Au-L3 NCSLs further suggests that NCSL growth occurs on the walls of capillaries, where the macroscopic orientation determines the microscopic lattice orientation (Figure 4a, S10). In the SAXS pattern of a horizontally set capillary, the indices indicate that the NCSLs have a close-packed (0001) facet against the wall (substrate), with the  $[1\bar{1}00]$  and  $[\bar{1}100]$  lattice vectors along the capillary (Figure 4b). Corresponding TEM images reveal the longer diagonal aligns with the  $[1\bar{1}00]$  lattice vectors, where the close-packed layers are perpendicular to the direction of the electron beam. During epitaxial growth on the capillary surfaces, close-packed layers are formed incrementally, and stacking faults may occur (Figure 4c). In situ SAXS observations of crystal growth highlight the emergence of a sharp HCP (1100) diffraction peak at the initial phase of NCSL growth. However, this peak diminishes progressively over time. In an increasingly thicker crystal, the FCC stacking faults disrupt the hexagonal symmetry, causing the HCP-exclusive peak to recede (Figure 4d). The average grain size along the vertical stacking direction reveals a fluctuating plateau stage between two incrementing growth stages, coinciding with the evolution and attenuation of the distinct (1100) peaks. This observation emphasizes the characteristic aspects of epitaxial growth.

The one-dimensional confinement of the capillary guides NCSL growth, with the front growing edges along the capillary exhibiting (1100) facets, resulting in a single-crystal-like diffraction pattern. Hexagonal or triangular plate shapes are also observed when slowly cooling the LC-NC dispersion on a flat substrate. In that case, the substrate dominates the out-of-plane orientation of NCSLs, while their in-plane orientation may vary. Due to the surface energy of the NCSL crystals, the well-faceted structure remains, leading to the persistence of similar shapes (Figure S7). In a vertically set capillary, mass transportation is constrained by the high viscosity of the LCs, causing the formation of Liesegang-like stripes for the as-formed NCSLs (Figure S5).<sup>48,49</sup> The recurring patterns indicate that the restricted inter-diffusion of NCs within LCs results in a macroscale self-regulation of periodic interfaces.<sup>50</sup> The formation mechanism of similar patterns in minerals and fluids remains a topic of debate, with our NCs in LCs presenting an innovative platform to address this fundamental puzzle.

This finding presents a novel approach to NCSL synthesis and can be extended and generalized to not only in different LCs, but also to NCs of diverse shapes, sizes, and materials. We explored alternative LCs as solvents to demonstrate this, such as 4-cyano-4'-octylbiphenyl (8CB), along with diverse NCs ranging in diameter from 5 nm to 15 nm. Nucleation continues to be triggered by the onset of isotropic to the LC phase transition, and resulting in the close-packed structures from the dispersion. Analogous to observations of Au in 5CB, these NCSLs can also have varied shapes and sizes which may go through different routes of nucleation and growth (Figure S13). The adaptability of the binding group on ligands to different NCs has been also demonstrated previously.<sup>47</sup>

In summary, we demonstrate the utility of LCs as a solvent for the on-demand cooling crystallization of NCs. The reversible and temperature-sensitive LC phase transition induces a solubility change in the NCs, offering another degree of freedom in manipulating NCSL growth. Ligand can impact the structures and behaviors of self-assembly with great tunability. Various routes of nucleation and growth lead to distinct morphologies and sizes of NCSLs. The abundance of different LCs, NCs, and surface ligands suggests diverse NCSL synthesis possibilities. The striking similarity between the NCSL growth in LC dispersion and the NC colloidal syntheses opens possible avenues for NCSL fabrication. Moreover, this approach reveals the dynamics of molecules during cooling crystallization. We anticipate this study will pave the way for 'colloidal synthesis' of NCSL clusters and liquid-phase epitaxy of mesoscale crystals.

## ASSOCIATED CONTENT

**Supporting Information.** Experimental details, additional experimental and simulation data, figures, and supplementary discussion (PDF).

## AUTHOR INFORMATION

### Corresponding Author

Christopher B. Murray [cbmurray@sas.upenn.edu](mailto:cbmurray@sas.upenn.edu)

### Author Contributions

S. Y. and Y. N. contributed equally.

### Notes

The authors declare no competing financial interest.

## ACKNOWLEDGMENT

The authors acknowledge primary support from NSF STC-IMOD under award DMR-2019444 and partial characterization support from the Office of Naval Research Multidisciplinary University Research Initiative (MURI) Award ONR N00014-18-1-2497. Y.N. acknowledges the support from NSF University of Pennsylvania Materials Research Science and Engineering Center (MRSEC) under awards DMR-1720530 for ligands synthesis. C.B.M. also acknowledges the Richard Perry University Professorship at the University of Pennsylvania. This research used resources of the Center for Functional Nanomaterials and the CMS beamline (11-BM) of the National Synchrotron Light Source II, both supported by the U.S. DOE Office of Science Facilities at Brookhaven National Laboratory under Contract No. DE-SC0012704. This work was carried out in part at the Singh Center for Nanotechnology, which is supported by the NSF National Nanotechnology Coordinated Infrastructure Program under grant NNCI-2025608. We thank Dr. R. Li and Dr. H. Zhang at NSLS-II for the help at the beamline and valuable discussions. We thank S. M. Thompson and C. Huang for their valuable suggestions.

## REFERENCES

- (1) Lee, M. S.; Yee, D. W.; Ye, M.; Macfarlane, R. J. Nanoparticle Assembly as a Materials Development Tool. *J. Am. Chem. Soc.* **2022**. <https://doi.org/10.1021/jacs.1c12335>.
- (2) Murray, C. B.; Kagan, C. R.; Bawendi, M. G. Self-Organization of CdSe Nanocrystallites into Three-Dimensional Quantum Dot Superlattices. *Science* **1995**, *270* (5240), 1335–1338.
- (3) Cherniukh, I.; Rainò, G.; Stöferle, T.; Burian, M.; Travesset, A.; Naumenko, D.; Amenitsch, H.; Erni, R.; Mahrt, R. F.; Bodnarchuk, M. I.; Kovalenko, M. V. Perovskite-Type Superlattices from Lead Halide Perovskite Nanocubes. *Nature* **2021**, *593* (7860), 535–542. <https://doi.org/10.1038/s41586-021-03492-5>.
- (4) Marino, E.; LaCour, R. A.; Moore, T. C.; van Dongen, S. W.; Keller, A. W.; An, D.; Yang, S.; Rosen, D. J.; Gouget, G.; Tsai, E. H. R.; Kagan, C. R.; Kodger, T. E.; Glotzer, S. C.; Murray, C. B. Crystallization of Binary Nanocrystal Superlattices and the Relevance of Short-Range Attraction. *Nat. Synth* **2023**, *1*–12. <https://doi.org/10.1038/s44160-023-00407-2>.
- (5) Diroll, B. T.; Jishkariani, D.; Cargnello, M.; Murray, C. B.; Donnio, B. Polycatenar Ligand Control of the Synthesis and Self-Assembly of Colloidal Nanocrystals. *J. Am. Chem. Soc.* **2016**, *138* (33), 10508–10515. <https://doi.org/10.1021/jacs.6b04979>.
- (6) Macfarlane, R. J.; Lee, B.; Jones, M. R.; Harris, N.; Schatz, G. C.; Mirkin, C. A. Nanoparticle Superlattice Engineering with DNA. *Science* **2011**, *334*, 204–208. <https://doi.org/10.1126/science.1210493>.
- (7) O'Brien, M. N.; Lin, H.-X.; Girard, M.; Olvera de la Cruz, M.; Mirkin, C. A. Programming Colloidal Crystal Habit with Anisotropic Nanoparticle Building Blocks and DNA Bonds.

- Journal of the American Chemical Society* **2016**, jacs.6b09704. <https://doi.org/10.1021/jacs.6b09704>.
- (8) Boles, M. A.; Engel, M.; Talapin, D. V. Self-Assembly of Colloidal Nanocrystals: From Intricate Structures to Functional Materials. *Chem. Rev.* **2016**, *116* (18), 11220–11289. <https://doi.org/10.1021/acs.chemrev.6b00196>.
- (9) Grzelczak, M.; Vermant, J.; Furst, E. M.; Liz-Marzán, L. M. Directed Self-Assembly of Nanoparticles. *ACS Nano* **2010**, *4* (7), 3591–3605. <https://doi.org/10.1021/nn100869j>.
- (10) Grzelczak, M.; Liz-Marzán, L. M.; Klajn, R. Stimuli-Responsive Self-Assembly of Nanoparticles. *Chem. Soc. Rev.* **2019**, *48* (5), 1342–1361. <https://doi.org/10.1039/C8CS00787J>.
- (11) Schlottheuber né Brunner, J.; Maier, B.; Thomä, S. L. J.; Kirner, F.; Baburin, I. A.; Lapkin, D.; Rosenberg, R.; Sturm, S.; Assalauova, D.; Carnis, J.; Kim, Y. Y.; Ren, Z.; Westermeier, F.; Theiss, S.; Borrmann, H.; Polarz, S.; Eychmüller, A.; Lubk, A.; Vartanyants, I. A.; Cölfen, H.; Zobel, M.; Sturm, E. V. Morphogenesis of Magnetite Mesocrystals: Interplay between Nanoparticle Morphology and Solvation Shell. *Chem. Mater.* **2021**, *33* (23), 9119–9130. <https://doi.org/10.1021/acs.chemmater.1c01941>.
- (12) Wang, Y.; Chen, J.; Li, R.; Götz, A.; Drobek, D.; Przybilla, T.; Hübner, S.; Pelz, P.; Yang, L.; Apeleo Zubiri, B.; Spiecker, E.; Engel, M.; Ye, X. Controlled Self-Assembly of Gold Nanotetrahedra into Quasicrystals and Complex Periodic Supracrystals. *J. Am. Chem. Soc.* **2023**, *145* (32), 17902–17911. <https://doi.org/10.1021/jacs.3c05299>.
- (13) Yee, D. W.; Lee, M. S.; An, J.; Macfarlane, R. J. Reversible Diffusionless Phase Transitions in 3D Nanoparticle Superlattices. *J. Am. Chem. Soc.* **2023**, *145* (11), 6051–6056. <https://doi.org/10.1021/jacs.3c01286>.
- (14) Marino, E.; Rosen, D. J.; Yang, S.; Tsai, E. H. R.; Murray, C. B. Temperature-Controlled Reversible Formation and Phase Transformation of 3D Nanocrystal Superlattices Through In Situ Small-Angle X-Ray Scattering. *Nano Lett.* **2023**, *23* (10), 4250–4257. <https://doi.org/10.1021/acs.nanolett.3c00299>.
- (15) Liu, Y.; Han, X.; He, L.; Yin, Y. Thermoresponsive Assembly of Charged Gold Nanoparticles and Their Reversible Tuning of Plasmon Coupling. *Angewandte Chemie International Edition* **2012**, *51* (26), 6373–6377. <https://doi.org/10.1002/anie.201201816>.
- (16) Brunner, J.; Maier, B.; Rosenberg, R.; Sturm, S.; Cölfen, H.; Sturm, E. V. Nonclassical Recrystallization. *Chemistry A European J* **2020**, *26* (66), 15242–15248. <https://doi.org/10.1002/chem.202002873>.
- (17) Kirner, F.; Sturm, E. V. Advances of Nonclassical Crystallization toward Self-Purification of Precious Metal Nanoparticle Mixtures. *Crystal Growth & Design* **2021**, *21* (9), 5192–5197. <https://doi.org/10.1021/acs.cgd.1c00544>.
- (18) Kang, Y.; Li, M.; Cai, Y.; Cargnello, M.; Diaz, R. E.; Gordon, T. R.; Wieder, N. L.; Adzic, R. R.; Gorte, R. J.; Stach, E. A.; Murray, C. B. Heterogeneous Catalysts Need Not Be so “Heterogeneous”: Monodisperse Pt Nanocrystals by Combining Shape-Controlled Synthesis and Purification by Colloidal Recrystallization. *J. Am. Chem. Soc.* **2013**, *135* (7), 2741–2747. <https://doi.org/10.1021/ja3116839>.
- (19) Zhang, Y.; Pal, S.; Srinivasan, B.; Vo, T.; Kumar, S.; Gang, O. Selective Transformations between Nanoparticle Superlattices via the Reprogramming of DNA-Mediated Interactions. *Nature Mater* **2015**, *14* (8), 840–847. <https://doi.org/10.1038/nmat4296>.
- (20) Kundu, P. K.; Samanta, D.; Leizrowice, R.; Margulis, B.; Zhao, H.; Börner, M.; Udayabhaskararao, T.; Manna, D.; Klajn, R. Light-Controlled Self-Assembly of Non-Photoresponsive Nanoparticles. *Nature Chem* **2015**, *7* (8), 646–652. <https://doi.org/10.1038/nchem.2303>.
- (21) Bian, T.; Gardin, A.; Gemen, J.; Houben, L.; Perego, C.; Lee, B.; Elad, N.; Chu, Z.; Pavan, G. M.; Klajn, R. Electrostatic Co-Assembly of Nanoparticles with Oppositely Charged Small Molecules into Static and Dynamic Superstructures. *Nat. Chem.* **2021**, *13* (10), 940–949. <https://doi.org/10.1038/s41557-021-00752-9>.
- (22) Mersmann, A. *Crystallization Technology Handbook*; Marcel Dekker Inc.: Hoboken, 2001.
- (23) Fu, H.; Gao, X.; Zhang, X.; Ling, L. Recent Advances in Non-classical Crystallization: Fundamentals, Applications, and Challenges. *Crystal Growth & Design* **2022**, *22* (2), 1476–1499. <https://doi.org/10.1021/acs.cgd.1c01084>.
- (24) Schlottheuber née Brunner, J. J.; Maier, B.; Kirner, F.; Sturm, S.; Cölfen, H.; Sturm, E. V. Self-Assembled Faceted Mesocrystals: Advances in Optimization of Growth Conditions. *Crystal Growth & Design* **2021**, *21* (10), 5490–5495. <https://doi.org/10.1021/acs.cgd.1c00507>.
- (25) Luo, B.; Wang, Z.; Curk, T.; Watson, G.; Liu, C.; Kim, A.; Ou, Z.; Luijten, E.; Chen, Q. Unravelling Crystal Growth of Nanoparticles. *Nat. Nanotechnol.* **2023**, *18* (6), 589–595. <https://doi.org/10.1038/s41565-023-01355-w>.
- (26) Huang, X.; Suit, E.; Zhu, J.; Ge, B.; Gerdes, F.; Klinke, C.; Wang, Z. Diffusion-Mediated Nucleation and Growth of Fcc and Bcc Nanocrystal Superlattices with Designable Assembly of Freestanding 3D Supercrystals. *J. Am. Chem. Soc.* **2023**, *145* (8), 4500–4507. <https://doi.org/10.1021/jacs.2c11120>.
- (27) Hegmann, T.; Qi, H.; Marx, V. M. Nanoparticles in Liquid Crystals: Synthesis, Self-Assembly, Defect Formation and Potential Applications. *J Inorg Organomet Polym* **2007**, *17* (3), 483–508. <https://doi.org/10.1007/s10904-007-9140-5>.
- (28) Qi, H.; Hegmann, T. Liquid Crystal–Gold Nanoparticle Composites. *Liquid Crystals Today* **2011**, *20* (4), 102–114. <https://doi.org/10.1080/1358314X.2011.610133>.
- (29) Jedrych, A.; Pawlak, M.; Gorecka, E.; Lewandowski, W.; Wojcik, M. M. Light-Responsive Supramolecular Nanotubes-Based Chiral Plasmonic Assemblies. *ACS Nano* **2023**, *17* (6), 5548–5560. <https://doi.org/10.1021/acsnano.2c10955>.
- (30) Pawlak, M.; Bagiński, M.; Lombart, P.; Beutel, D.; González-Rubio, G.; Górecka, E.; Rockstuhl, C.; Mieczkowski, J.; Pocięcha, D.; Lewandowski, W. Tuneable Helices of Plasmonic Nanoparticles Using Liquid Crystal Templates: Molecular Dynamics Investigation of an Unusual Odd–Even Effect in Liquid Crystalline Dimers. *Chem. Commun.* **2022**, *58* (53), 7364–7367. <https://doi.org/10.1039/D2CC00560C>.
- (31) Rodarte, A. L.; Pandolfi, R. J.; Ghosh, S.; Hirst, L. S. Quantum Dot/Liquid Crystal Composite Materials: Self-Assembly Driven by Liquid Crystal Phase Transition Templating. *J. Mater. Chem. C* **2013**, *1* (35), 5527–5532. <https://doi.org/10.1039/C3TC31043D>.
- (32) Milette, J.; Cowling, S. J.; Toader, V.; Lavigne, C.; Saez, I. M.; Lennox, R. B.; Goodby, J. W.; Reven, L. Reversible Long Range Network Formation in Gold Nanoparticle - Nematic Liquid Crystal Composites. *Soft Matter* **2011**, *8* (1), 173–179. <https://doi.org/10.1039/C1SM06604H>.
- (33) West, J. L.; Zhang, K.; Liao, G.; Reznikov, Y.; Andrienko, D.; Glushchenko, A. V. Mechanism of Formation of Three Dimensional Structures of Particles in a Liquid Crystal. *Journal of Information Display* **2002**, *3* (3), 17–23. <https://doi.org/10.1080/15980316.2002.9651896>.
- (34) Bi, Y.; Cheng, C.; Zhang, Z.; Liu, R.; Wei, J.; Yang, Z. Controlled Hierarchical Self-Assembly of Nanoparticles and Chiral Molecules into Tubular Nanocomposites. *J. Am. Chem. Soc.* **2023**, *145* (15), 8529–8539. <https://doi.org/10.1021/jacs.3c00636>.
- (35) Yang, Y.; Liu, C.; Ding, Y.; Ding, B.; Xu, J.; Liu, A.; Yu, J.; Grater, L.; Zhu, H.; Hadke, S. S.; Sangwan, V. K.; Bati, A. S. R.; Hu, X.; Li, J.; Park, S. M.; Hersam, M. C.; Chen, B.; Nazee-ruddin, M. K.; Kanatzidis, M. G.; Sargent, E. H. A Thermotropic Liquid Crystal Enables Efficient and Stable Perovskite Solar Modules. *Nat Energy* **2024**, 1–8. <https://doi.org/10.1038/s41560-023-01444-z>.
- (36) Rodarte, A. L.; Cao, B. H.; Panesar, H.; Pandolfi, R. J.; Quint, M.; Edwards, L.; Ghosh, S.; Hein, J. E.; Hirst, L. S. Self-Assembled Nanoparticle Micro-Shells Templated by Liquid

- Crystal Sorting. *Soft Matter* **2015**, *11* (9), 1701–1707. <https://doi.org/10.1039/C4SM02326A>.
- (37) Mac Fhionnlaioich, N.; Schrettl, S.; Tito, N. B.; Yang, Y.; Nair, M.; Serrano, L. A.; Harkness, K.; Silva, P. J.; Frauenrath, H.; Serra, F.; Carter, W. C.; Stellacci, F.; Guldin, S. Reversible Microscale Assembly of Nanoparticles Driven by the Phase Transition of a Thermotropic Liquid Crystal. *ACS Nano* **2023**, *acs.nano.2c09203*. <https://doi.org/10.1021/acs.nano.2c09203>.
- (38) Prodanov, M. F.; Pogorelova, N. V.; Kryshchal, A. P.; Klymchenko, A. S.; Mely, Y.; Semynozhenko, V. P.; Krivoshey, A. I.; Reznikov, Y. A.; Yarmolenko, S. N.; Goodby, J. W.; Vashchenko, V. V. Thermodynamically Stable Dispersions of Quantum Dots in a Nematic Liquid Crystal. *Langmuir* **2013**, *29* (30), 9301–9309. <https://doi.org/10.1021/la401475b>.
- (39) Lavrentovich, O. D. Transport of Particles in Liquid Crystals. *Soft Matter* **2014**, *10* (9), 1264–1283. <https://doi.org/10.1039/C3SM51628H>.
- (40) Škarabot, M.; Tkalec, U.; Muševič, I. Transport and Crystallization of Colloidal Particles in a Thin Nematic Cell. *Eur. Phys. J. E* **2007**, *24* (1), 99–107. <https://doi.org/10.1140/epje/i2007-10218-0>.
- (41) Dong, A.; Chen, J.; Vora, P. M.; Kikkawa, J. M.; Murray, C. B. Binary Nanocrystal Superlattice Membranes Self-Assembled at the Liquid–Air Interface. *Nature* **2010**, *466* (7305), 474–477.
- (42) Yang, S.; LaCour, R. A.; Cai, Y.-Y.; Xu, J.; Rosen, D. J.; Zhang, Y.; Kagan, C. R.; Glotzer, S. C.; Murray, C. B. Self-Assembly of Atomically Aligned Nanoparticle Superlattices from Pt–Fe<sub>3</sub>O<sub>4</sub> Heterodimer Nanoparticles. *J. Am. Chem. Soc.* **2023**, *145* (11), 6280–6288. <https://doi.org/10.1021/jacs.2c12993>.
- (43) Ning, Y.; Liu, Z.; Yang, S.; Morimitsu, Y.; Osuji, C. O.; Murray, C. B. Design of Dendritic Promesogenic Ligands for Liquid Crystal–Nanoparticle Hybrid Systems. *Chem. Mater.* **2023**, *35* (9), 3532–3544. <https://doi.org/10.1021/acs.chemmater.3c00057>.
- (44) Ohring, M. *Materials Science of Thin Films: Deposition and Structure*, 2nd ed.; Academic Press: San Diego, CA, 2002.
- (45) Liu, M.; Fu, J.; Yang, S.; Wang, Y.; Jin, L.; Nah, S. H.; Gao, Y.; Ning, Y.; Murray, C. B.; Yang, S. Janus Microdroplets with Tunable Self-Recoverable and Switchable Reflective Structural Colors. *Advanced Materials* **2023**, *35* (5), 2207985. <https://doi.org/10.1002/adma.202207985>.
- (46) Gu, J.; Zhang, Y.-W.; Franklin (Feng) Tao. Shape Control of Bimetallic Nanocatalysts through Well-Designed Colloidal Chemistry Approaches. *Chemical Society Reviews* **2012**, *41* (24), 8050–8065. <https://doi.org/10.1039/C2CS35184F>.
- (47) Ning, Y.; Yang, S.; Yang, D.-B.; Cai, Y.-Y.; Xu, J.; Li, R.; Zhang, Y.; Kagan, C. R.; Saven, J. G.; Murray, C. B. Dynamic Nanocrystal Superlattices with Thermally-Triggerable Lubricating Ligands. *Journal of the American Chemical Society In Press*. <https://doi.org/10.1021/jacs.3c10706>.
- (48) Akbulut, E. S.; Holló, G.; Lagzi, I.; Baytekin, B. Complex Patterning of Matter with Liesegang Patterns Propagating through Different Concentration Media—Gel Lenses for Liesegang Waves. *Crystal Growth & Design* **2023**, *acs.cgd.3c00871*. <https://doi.org/10.1021/acs.cgd.3c00871>.
- (49) Nabika, H.; Itatani, M.; Lagzi, I. Pattern Formation in Precipitation Reactions: The Liesegang Phenomenon. *Langmuir* **2020**, *36* (2), 481–497. <https://doi.org/10.1021/acs.langmuir.9b03018>.
- (50) Dong, A.; Chen, J.; Oh, S. J.; Koh, W.; Xiu, F.; Ye, X.; Ko, D.-K.; Wang, K. L.; Kagan, C. R.; Murray, C. B. Multiscale Periodic Assembly of Striped Nanocrystal Superlattice Films on a Liquid Surface. *Nano Lett.* **2011**, *11* (2), 841–846. <https://doi.org/10.1021/nl104208x>.

Insert Table of Contents artwork here

